18

Highly Compliant Bonding Material for Micro- and Opto-Electronic Applications

E. Suhir[a] and D. Ingman[b]

[a]*University of California, Santa Cruz, CA, University of Maryland, College Park, MD, USA*
[b]*Technion, Israel*

18.1. INTRODUCTION

Bonded assemblies (joints) that experience thermal and/or mechanical loading are widely used in micro- and opto-electronics. These assemblies are typically subjected to thermal stresses due to the thermal expansion (contraction) mismatch of the dissimilar materials of the adherends and/or because of temperature gradients. In other cases, bonded assemblies experience mechanical loading. It has been established that the most reliable adhesively bonded or soldered assemblies are characterized by stiff adherends and a compliant adhesive. It has been established also that the employment of low modulus bonding materials and thick bonding layers can lead to an appreciable stress relief [1–7]. This is true for both the interfacial stresses (which are responsible for the adhesive and the cohesive strength of the bonding material) and the stresses acting in the cross-sections of the adherends (these stresses are responsible for the strength of the bonded components) [8–10]. Since the interfacial stresses concentrate at the assembly ends, a substantial stress relief could be expected, if a low modulus material is used at the peripheral portions of the joint [11,12]. Low modulus and thick (up to 4 mils or even thicker) bonding layers are currently employed in micro- and opto-electronic packaging in order to provide a desirable strain buffer between the adherend materials. Certainly, there is always a need in the art for better bonding materials that combine good adhesive properties with high interfacial compliance.

In this connection it should be point out that the reliability of a bonded assembly is due to both high bearing capacity of the joint (i.e., its ability to withstand high stresses of any nature, as well as repetitive loading) and to the low enough level of loading. High compliance of the bonding layer is aimed at reducing the level of the loading, thereby making sufficiently reliable even those joints whose bearing capacity might not be very high. It is also noteworthy that in "conventional" assemblies (which are characterized by moderately compliant bonding layers), the interfacial compliance is due to both the bonding

layer and the bonded components. It is not advisable, however, and, in many cases, is not even possible, to increase the interfacial compliance of the adherends. The most attractive way to increase the interfacial compliance and, hence, the reliability of a bonded joint is to employ a highly compliant, yet thin enough (say, for lower thermal resistance) bonding layer. In assemblies with highly compliant bonds, the role of the adherends, as far as the interfacial compliance is concerned, is insignificant. It is the bonding material only that is responsible for the high and favorable interfacial compliance.

In this chapter we suggest an analytical stress model that enables one to quantitatively assess the expected relief in the interfacial shearing stress due to the application of a highly compliant bonding layer. We use this model to demonstrate that the application of a wire array (WA) and/or a suitable modification of a newly developed nano-particle material (NPM) and structure can improve dramatically the compliance of a bonding layer. This NPM has extraordinary mechanical and environmental properties [13–15]. It has been recently tested in application to a new generation of cladding and coatings for fiber optic systems [16–18]. We expect that this material will find a wide application in micro- and opto-electronics, and beyond.

18.2. EFFECT OF THE INTERFACIAL COMPLIANCE ON THE INTERFACIAL SHEARING STRESS

The objective of the developed analytical stress model (see Appendix 18.A) is to evaluate the effect of the interfacial compliance on the interfacial shearing stress. We use this model to demonstrate the importance of highly compliant bonds. This could certainly be done in addition to, or sometime even instead of, employing adherends with a good thermal extension (contraction) match. The following major conclusions can be drawn from the analysis based on the developed model.

The interfacial shearing stress is proportional to the parameter of the interfacial compliance. This parameter is defined as a square root of the ratio of the axial compliance of the assembly (which, in typical assemblies with thin and/or low modulus bonds, is due to the adherends only and should be made as low as possible) to the assembly's interfacial compliance (which, in typical assemblies is due to both the adherends and the bonding layer). In "conventional" assemblies, i.e., in assemblies with a moderately compliant bonding layer, the interfacial compliance is due to both the adherends and the adhesive: thick and high-modulus adherends and a thin and low-modulus adhesives typically contribute more or less equally to the total interfacial compliance. If, however, a highly compliant bonding layer is employed, it is only this layer, and not the adherends, that is responsible for the interfacial compliance of the bond, and, hence, for the structural reliability of the joint.

Although the predictive model was developed for a "flat" (planar) joint, the above conclusions are valid for any assembly, whether circular (e.g., in fiber optics applications), flat (as in microelectronics applications), elliptical, etc.

The level of stress relief that could be expected by employing a WA as a compliant attachment can be assessed based on the following simple reasoning. Examine a bonded structure, in which the bonding layer is constructed of an array of wires, particularly, nanowires. Let the wires have circular cross-sections and can be considered rigidly clamped at

the ends. Treating each wire as a beam clamped at its ends and experiencing ends offset of the magnitude δ, we find that the lateral forces at the wire ends are

$$N = 12 \frac{EI\delta}{h_0^3} = \frac{3\pi}{16} \frac{Ed^4\delta}{h_0^3}, \tag{18.1}$$

where E is the Young's modulus of the wire material, d is the wire diameter, and h_0 is the wires' height, i.e., the thickness of the WA (bonding layer). In the Equation (18.1),

$$I = \frac{\pi \cdot d^2}{64}$$

is the moment of inertia of the wire cross-section. The interfacial compliance of the bonding layer can be found by multiplying the δ/N ratio by the wire cross-sectional area

$$A = \frac{\pi \cdot d^2}{4}. \tag{18.2}$$

This results in the following formula for the interfacial compliance:

$$\kappa_w = \frac{16h_0^3}{3\pi Ed^4} \frac{\pi d^2}{4} = \frac{4}{3} \frac{h_0^3}{Ed^2}. \tag{18.3}$$

Using the Equation (18.A7) for the interfacial compliance of a "conventional" (adhesively bonded or soldered) assembly, we conclude that the ratio

$$\eta = \frac{4}{3} \frac{G_0}{E} \left(\frac{h_0}{d} \right)^2 \tag{18.4}$$

could be used to assess the advantage of a WA-based bonding layer in comparison with a "conventional" layer. Let, for instance, a conventional bonding material has a shear modulus of 5000 psi, the Young's modulus of the WA material be $E = 15 \times 106$ psi, the thickness of the bonding layer be $h_0 = 50$ μm, and the diameter of a single wire be 100 nm. Then the Equation (18.4) yields: $\eta = 111$. Hence, a significant increase in the interfacial compliance could be expected by using a WA-based bonding structure, and, because the interfacial shearing stress is inversely proportional to the square root of the interfacial compliance, one could expect an order of the magnitude decrease in the interfacial shearing stress.

Although the above analysis was carried out for a "clamped-clamped" wire, the results are equally applicable to wires with other boundary conditions at the ends. Additional increase in the interfacial compliance could be achieved, if the wires experience axial compression. In order to assess the expected effect of such a compression, we have examined, as an illustration, in Appendix 18.B, a cantilever wire (beam) subjected at its free end to a lateral (bending) force, P, and an axial compressive force, T. The force P can produce a significantly larger lateral deflection, if the wire is subjected to an external axial compression. Such an effect should be expected, of course, since a compressed wire (beam) experiences lateral deflections even in the absence of any lateral force, provided that the axial force reaches and exceeds its critical value.
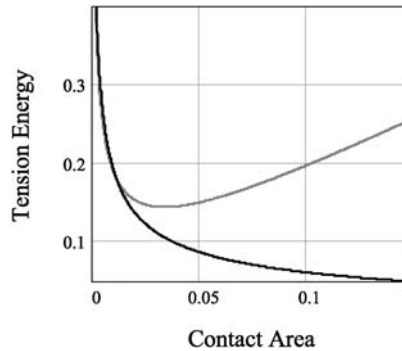
FIGURE 18.1. Surface potential energy vs. "bonded" surface-compound (adhesion) area. Red line — $\sigma_{SC} > \sigma_{SA}$ Blue line — $\sigma_{SC} < \sigma_{SA}$ (see Appendix 18.C).

18.3. INTERNAL COMPRESSIVE FORCES

In addition to the external compression that can be imposed deliberately to enhance the lateral compliance of the assembly, there exist also "internal" compressive forces caused by surface tension.

Consider two bonding surfaces (e.g., parallel surfaces, although these surfaces do not have to be necessarily parallel) and a certain amount of the bonding material (compound) that touches the bonded surfaces. Let us suppose, for the sake of simplicity, that this bonding compound has a shape of a circular cylinder, whose bases touch the bonded surfaces. The lateral surface of the cylinder is "free," i.e., is in contact with air. Let us address a situation, when the area of each of the two bonded surfaces is greater than the bonding area, i.e., the area of the contact with the bonding material. If the surface tension characteristics of the bonding and the bonded materials are properly chosen, then the attraction forces will arise between the bonding surfaces. This phenomenon is similar to the phenomenon observed during the formation of solder balls. So, the bonding compound material will tend to decrease its "free" area and increase its contact area with the bonded surfaces. The total volume of the cylinder remains unchanged. Such a "self-adjusting" process stops when the potential energy of the system (which is as a function of the distance between the bonded surfaces) becomes minimal. A typical plot for this potential energy vs. the contact area is shown in Figure 18.1. The development of the expression for the potential energy is given in the Appendix 18.C.

If the distance between the bonded surfaces becomes larger than the minimum distance that corresponds to the minimum strain energy of the system, then the bonding material behaves as a, sort of, a stretched spring, trying to bring the bonded surfaces closer, i.e., providing axial compression. This compression is proportional to the derivative of the elastic energy with respect to the distance between the bonded surfaces.

18.4. ADVANCED NANO-PARTICLE MATERIAL (NPM)

NPM is an unconventional inhomogeneous "smart" composite material that is equivalent to a "hypothetical" homogeneous material with the following major properties:

- Low Young's modulus.
- Immunity to corrosion.

- Good adhesion to the adjacent material.
- Non-volatile.
- Stable properties at temperature extremes (from $+350°C$ to as low as $-220°C$).
- Very long (practically infinite) lifetime.
- Strong hydrophobicity (against both water and water vapor).
- Ability for "self-healing:" ability to restore its dimensions and initial structure when damaged.
- Ability for "healing" the surfaces of the adjacent materials, i.e., to fill in the existing and/or the developed defects (surface cracks, flaws, and other imperfections) and to slow down their propagation and/or even to "arrest" them completely.
- Very low effective refractive index (if needed).
- High dielectric constant (if needed).

The NPM can be designed, depending on the particular application, in such a way that its important particular properties are enhanced. The conducted tests have confirmed these properties. In general, it is desirable to provide application-specific modifications of the NPM to master (optimize) its properties and performance. Because it is a nano-material, its surface chemistry and its performance depend a lot upon the contact materials and surfaces. The NPM applications include, but are not limited, to the following ones:

- Hermetic sealing of packages, components and devices, such as laser packages, MEMS, displays, plastic LEDs, etc.
- Effective protection (coating) for various metal and non-metal surfaces, well beyond the area of micro- and opto-electronic packaging: (cars, aerospace structures, off-shore and ocean structures, marine vehicles, bridges, towers, tubes, pipes and pipe-lines, etc.). These applications benefit because the NPM is actively hydrophobic, does not induce additional stresses (owing to its low modulus), is inexpensive, is easy-to-apply, has practically infinite lifetime, and is self-healing. Application of the NPM can result in a significant resistance of a metal surface to corrosion, and, in addition, in substantial increase in the fracture toughness of the material, both initially and during the system's operation (use).
- The NPM can be added in the formulation of various coatings such as paints, thereby providing protective benefits without changing the application techniques.
- Because of a low refractive index, the NPM can be used, if necessary, as an effective cladding of optical silica fibers. The use of the NPM cladding eliminates the need to dope silica for obtaining light-guide cores. The new preform will consist of a single (undoped and, hence, less expensive) silica material.
- A derivative application is flexible light-guides. Multicore flexible fiber cables employing NPM are able to provide high spatial image resolution. As such, they might find important applications, when there is a need to provide direct high-resolution image transmission from secluded areas. Possible applications can be found in bio-medicine, nondestructive evaluations, oil and other geological explorations, in ocean engineering, or in other situations when an image needs to be obtained and transmitted from relatively inaccessible locations.
- Another derivative application is a multicore fiber cable. Ultra-small diameter glass fibers with an NPM-based cladding/coating can be placed in large quantities within a NPM medium ("multiple cores in a single cladding"). In addition, owing to a much better inner-outer refractive index ratio in the NPM-based fibers, such cables will be characterized by very low signal attenuation.

- Yet another derivative application is sensor systems. The NPM-based fibers can be used in optical sensor systems that employ optical fibers embedded in a laminar or a cast material. Such systems are used, for instance, in composite airframes. With the NPM used as a cladding or, at least, as a coating of the silica optical fiber, the optical performance, the mechanical reliability and the environmental durability of the light-guide will be improved dramatically compared to the conventional systems.
- Ultra-thin planar light-guides are yet another derivative application of the NPM. In the new generation of the planar light-guides, NPM can be used as the top cladding material. It will replace silicon or polymer claddings, which are considered in today's planar light-guides. All the advantages of the NPM cladding material discussed above for optical fibers are equally applicable to planar light-guides. These are thought to have a "bright" future in the next generation of computers and other photonic devices.

18.5. HIGHLY-COMPLIANT NANO-SYSTEMS

In the current application, intended primarily for micro- and opto-electronic assemblies, we have developed a modification of the NPM for use as a highly compliant bonding structure. Here are some major characteristics of this material (additional to those described in the previous section).

The NPM for the application in question is highly inhomogeneous, anisotropic and thixotropic. It allows for an elevated, but still limited displacement in the in-plane direction, i.e., in the direction of the interfacial shearing stress. The material includes a filler and nanoparticles. The bonding elements are of a "strings-like" structural type. These elements are slightly compressed in the through-thickness direction. This enhances their compliance (flexibility) in the in-plane direction. The thixotropic matrix is quasi-solid in the absence of the applied stress field (disturbance) and becomes much less viscous and even quasi-liquid, when thermal or mechanical stress is applied. In other words, the bonding structure becomes much more compliant as a result of experiencing mechanical or thermal loading. The structure provides a highly effective strain buffer between the adherends.

The role of such a plurality of links (strings) are played by numerous nanotubes and/or nanowires embedded into the bonding matrix. Nanotubes and/or nanowires could be subjected to externally and/or internally deliberately induced compression in the through-thickness direction for even higher lateral compliance. In bonded structures of a circular (such as coated optical fibers or cables) or elliptic shape, the radial compression (hoop stresses) arises because of the thermal contraction mismatch in the radial direction of the high CTE coating and low CTE cladding. In flat (planar) bonded joints the compression in the through-thickness direction could be introduced deliberately (externally or internally).

The filler of the bonding compound has to have a high wetting ability with respect to the bonded surfaces. This means that the surface tension at the interface between the bonding compound (structure) and the bonded surface has to be much lower, than at the "free" surface of the bond. This allows for creating the desirable distance-depending attraction forces

In order to keep the system at the near-optimal distance between the bonded surfaces, the NPM-based compound has to maintain the adequate gap between the surfaces. This can be achieved by introducing microspheres into the compound. Such micro-spheres could serve as, sort of, bearing rolls that increase the system's stability and provide the desirable anisotropy of bonding matrix.
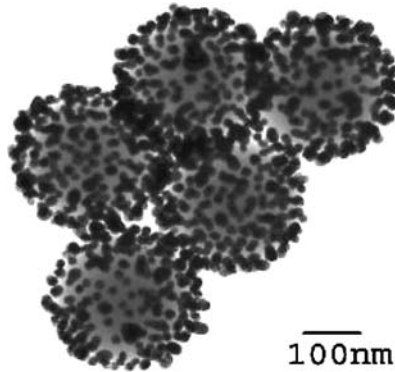
FIGURE 18.2. Microspheres with "protrusions."

The highly-compliant nano-systems in question are extremely heterogeneous. They consist of a bonding matrix with numerous embedded nanoparticles, microspheres and nanotubes/nanowires (whiskers). All these nano- and micro-particles embedded into a thixotropic matrix enable one to create a multi-purpose thixotropic structure. Figure 18.2 illustrates a possible combination of microspheres with "protrusions." These "protrusions" are formed by surface nanoparticles' clusters attracted to the microspheres.

18.6. CONCLUSIONS

The following conclusions can be drawn from the carried out analysis:

- Based on the developed simplified analytical stress model, we demonstrated that the employment of highly compliant materials and structures as bonding layers in bimaterial assemblies (joints) can lead to a significant relief in both the thermally induced and mechanical stresses. The model indicates that the interfacial shearing stress in an adhesively bonded or a soldered assembly is inversely proportional to the square root of the interfacial compliance, and that in "conventional" bimaterial assemblies (which are characterized by not-highly-compliant bonding layers), the interfacial compliance is due to both the bonding layer and the bonded components themselves. However, in assemblies with highly compliant bonds, it is the bonding material only that provides the high and favorable interfacial compliance.
- An appropriate wire array (WA) fabricated on one or both bonded components can be used as a suitable compliant bond. Based on the developed stress model, we demonstrate that its application can lead to a significant, about two orders of magnitude, increase in the interfacial compliance, thereby leading to a reduction in the maximum interfacial shearing stress of about an order of magnitude (compared to the bonded joints using "conventional" adhesives or solders).
- A modification of the newly developed nano-particle material (NPM) be used to increase dramatically the compliance of the bonding layer.
- The combination of both approaches could be effectively used to provide a highly compliant and a highly reliable bonding material and structure. In this case the NPM is employed as a suitable embedding material for the WA.
- Since the NPM has extraordinary mechanical and environmental properties, and, in combination with the appropriate WA, can make an extremely highly compliant

bond, we expect that the NPM and WA, used independently or in combination, might find a wide application in assemblies employed in micro- and opto-electronics, and beyond.

REFERENCES

1. E. Suhir, Thermal stress failures in microelectronics and photonics: prediction and prevention, Future Circuits International, (5) (1999).
2. E. Suhir, Buffering effect of fiber coating and its influence on the proof-test load in optical fibers, Applied Optics, 29(18) (1990).
3. Z. Kovac, et al., Compliant interface for semiconductor chip and method therefor, U.S. Patent #6,133,639, 2000.
4. T.H. DiStefano, et al., Compliant microelectronic mounting device, U.S. Patent #6,370,032, 2002.
5. Z. Kovac, et al., Methods for making electronic assemblies including compliant interfaces, U.S. Patent #6,525,429, 2003.
6. E. Paterson, et al., Mechanical highly compliant thermal interface pad, U.S. Patent #6,910,271, 2005.
7. Z. Kovac, et al., Methods of making microelectronic assemblies including compliant interfaces, U.S. Patent #6,870,272, 2005.
8. E. Suhir, Stresses in bi-metal thermostats, ASME Journal of Applied Mechanics, 53(3) (1986).
9. E. Suhir, Calculated thermally induced stresses in adhesively bonded and soldered assemblies, Proc. of the Int. Symp. on Microelectronics, ISHM, 1986, Atlanta, Georgia, Oct. 1986.
10. E. Suhir, Interfacial stresses in bi-metal thermostats, ASME Journal of Applied Mechanics, 56(3) (1989).
11. E. Suhir, Thermal stress in a polymer coated optical glass fiber with a low modulus coating at the ends, Journal of Materials Research, 16(10) (2001).
12. E. Suhir, Thermal stress in an adhesively bonded joint with a low modulus adhesive layer at the ends, Applied Physics Journal, (April) (2003).
13. E. Suhir, New nano-particle material (NPM) for micro- and opto-electronic packaging applications, IEEE Workshop on Advanced Packaging Materials, Irvine, March 2005.
14. D. Ingman and E. Suhir, Optical fiber with nanoparticle cladding, Patent Application, 2001 (allowed).
15. D. Ingman, V. Ogenko, and E. Suhir, Moisture-resistant nano-particle material and its applications, Patent Application, 2003 (pending).
16. E. Suhir, New hermetic coating for optical fiber dramatically improves strength, DARPA and Navair Workshop, St. Louis, MO, August 2004.
17. E. Suhir, Polymer coated optical glass fiber reliability: could nano-technology make a difference? Polytronic'04, Portland, OR, September 13–15, 2004.
18. E. Suhir, Mechanics of coated optical fibers: review and extension, ECTC'2005, Orlando, Florida, 2005.

APPENDIX 18.A. BIMATERIAL ASSEMBLY SUBJECTED TO AN EXTERNAL SHEARING LOAD AND CHANGE IN TEMPERATURE: EXPECTED STRESS RELIEF DUE TO THE ELEVATED INTERFACIAL COMPLIANCE

The following major assumptions are used in the analysis:

- Approximate methods of structural analysis (strength-of-materials) and materials science, rather than methods of elasticity, can be used to evaluate stresses and displacements.
- The bonded components can be treated, from the standpoint of structural analysis, as elongated rectangular strips that experience linear in-plane elastic deformations.
- At least one of the components ("substrate") is thick (stiff) enough so that bending deformations of the assembly as a whole do not occur and need not be considered.
- All the materials can be treated as linearly elastic.

- The interfacial shearing stresses can be evaluated based on the concept of the inter-facial compliance, without considering the effect of the "peeling" stresses (normal interfacial stresses acting in the through-thickness direction).

Let a bimaterial assembly be subjected to both an external shearing force, $\widehat{T}$, and change, Δt, in temperature. Assuming, for instance, that the assembly was manufactured at an elevated temperature and subsequently cooled down to a low (say, room) temperature, one can seek, in an approximate analysis, the longitudinal interfacial displacements, $u_1(x)$ and $u_2(x)$, of the assembly components #1 and #2, respectively, in the form:

$$u_1(x) = -\alpha_1 \Delta t x + \lambda_1 \int_0^x T(\xi)d\xi - \kappa_1 \tau(x),$$

$$u_2(x) = -\alpha_2 \Delta t x - \lambda_2 \int_0^x T(\xi)d\xi + \kappa_{21} \tau(x).$$
(18.A1)

In this equations, α_1 and α_2 are the coefficients of thermal expansion (CTEs) of the dissimilar materials,

$$\lambda_1 = \frac{1 - \nu_1}{E_1 h_1}, \quad \lambda_2 = \frac{1 - \nu_2}{E_2 h_2}$$
(18.A2)

are the axial compliances of the assembly components, E_1 and E_2 are the Young's moduli of the materials, ν_1 and ν_2 are their Poisson's ratios, h_1 and h_2 are the thicknesses of the assembly components,

$$T(x) = x \int_{-l}^x \tau(\xi)d\xi$$
(18.A3)

are the thermally induced forces acting in the cross-sections of the assembly components, $\tau(x)$ is the thus far unknown interfacial shearing stress, l is half the assembly length,

$$\kappa_1 = \frac{h_1}{3G_1}, \quad \kappa_2 = \frac{h_2}{3G_2}$$
(18.A4)

are the interfacial compliances of the assembly components, and

$$G_1 = \frac{E_1}{2(1 + \nu_1)}, \quad G_2 = \frac{E_2}{2(1 + \nu_2)}$$
(18.A5)

are the shear moduli of the adherend materials. The origin, O, of the coordinate, x, is at the mid-cross-section of the assembly. The condition of the compatibility of the longitudinal interfacial displacements (18.A1) can be written as follows:

$$u_1(x) = u_2(x) - \kappa_0 \tau(x),$$
(18.A6)

where

$$\kappa_0 = \frac{h_0}{G_0} = 2(1 + \nu_0)\frac{h_0}{E_0}$$
(18.A7)

is the interfacial compliance of the bonding layer, h_0 is the thickness of this layer, E_0 and ν_0 are the elastic constants of the bonding material, and G_0 is its shear modulus. Introducing the Equation (18.A1) into the compatibility condition (18.A6), we obtain the following equation for the sought interfacial shearing stress function, $\tau(x)$:

$$\kappa \tau(x) - \lambda \int_0^x T(\xi)d\xi = \Delta\alpha\Delta t x, \tag{18.A8}$$

where

$$\kappa = \kappa_0 + \kappa_1 + \kappa_2 \tag{18.A9}$$

is the total interfacial compliance of the assembly,

$$\lambda = \lambda_1 + \lambda_2 \tag{18.A10}$$

is the total axial compliance, and $\Delta\alpha = \alpha_1 - \alpha_2$ is the thermal contraction mismatch of the adherend materials.

Differentiating the Equation (18.A8) with respect to the coordinate, x, we obtain:

$$\kappa \tau'(x) - \lambda T(x) = \Delta\alpha\Delta t. \tag{18.A11}$$

The next differentiation, taking into account the Equation (18.A3), yields:

$$\kappa \tau''(x) - \lambda T(x) = 0. \tag{18.A12}$$

The boundary conditions

$$T(-l) = 0, \qquad T(l) = \widehat{T} \tag{18.A13}$$

for the induced force can be translated, using the Equation (18.A11), into the boundary conditions for the interfacial shearing stress, $\tau(x)$, as follows:

$$\tau'(-l) = \frac{\Delta\alpha\Delta t}{\kappa}, \quad \tau'(l) = \frac{\Delta\alpha\Delta t + \lambda\,\widehat{T}}{\kappa}. \tag{18.A14}$$

Equation (18.A12) has the following solution:

$$\tau(x) = C_1 \sinh kx + C_2 \cosh kx, \tag{18.A15}$$

where

$$k = \sqrt{\frac{\lambda}{\kappa}} \tag{18.A16}$$

is the parameter of the interfacial sharing stress. Introducing the solution (18.A15) into the boundary conditions (18.A14), solving the obtained equations for the constants C_1

and C_2 of integration, and substituting the formulas for the constants of integration into the solution (18.A15), we obtain the following expression for the interfacial shearing stress:

$$\tau(x) = k \left\{ \frac{\Delta\alpha\,\Delta t}{\lambda} \frac{\sinh kx}{\cosh kl} + \hat{T} \frac{\cosh[k(x+l)]}{\sinh 2kl} \right\}. \tag{18.A17}$$

The maximum value of this stress occurs, in this simplified stress model, at the end $x = l$:

$$\tau_{\max} = \tau(l) = k \left(\frac{\Delta\alpha\,\Delta t}{\lambda} \tanh kl + \hat{T} \coth 2kl \right). \tag{18.A18}$$

In sufficiently long and/or stiff assemblies, this formula yields:

$$\tau_{\max} = \tau(l) = k \left(\frac{\Delta\alpha\,\Delta t}{\lambda} + \hat{T} \right). \tag{18.A19}$$

Thus, it is the parameter, k, of the interfacial shearing stress that is responsible for both the level of this stress and the length of the end portions of the assembly that experience elevated interfacial stresses. As evident from the Equation (18.A16), this parameter decreases with a decrease in the axial compliance, λ, of the assembly and with an increase in the assembly's interfacial compliance κ. The axial compliance, λ, as evident from the Equations (18.A2), is due to the adherends only, and it is desirable, as evident from the Equation (18.A6), that these adherends are stiff, i.e., are characterized by a low axial compliance. As to the interfacial compliance, κ, this compliance, for conventional assemblies with not a very compliant bonding layer, is due to both the interfacial compliance of the bonding layer and the adherends themselves: the bonding layer is typically thin and low modulus, while the adherends are thick and high modulus, so, as evident from the Equations (18.A4) and (18.A7), the contribution of the compliances of the adherends and the bonding layer to the total compliance expressed by the Equation (18.A9), might be quite comparable. From the obtained formulas it is clear also that there is no incentive to increase the interfacial compliance of the adherends: by doing so, one would inevitably increase the axial compliance of the assembly as well, which is highly undesirable. Hence, for lower interfacial shearing stress, one should design a joint with a highly compliant bonding layer. This will make the factor k lower, will bring down the maximum interfacial shearing stress (which is inversely proportional to the square root of the interfacial compliance) and will spread the interfacial shearing loading over larger areas at the assembly ends.

APPENDIX 18.B. CANTILEVER WIRE ("BEAM") SUBJECTED AT ITS FREE END TO A LATERAL (BENDING) AND AN AXIAL (COMPRESSIVE) FORCE

Let a cantilever wire ("beam") be subjected at its free end to a lateral (bending) force, P, and an axial compressive force, T. The equation of bending of such a beam is as follows:

$$EIw''(x) + Tw(x) = 0. \tag{18.B1}$$

Here $w(x)$ is the deflection function of the beam, and EI is its flexural rigidity. The origin, O, of the coordinate x is at the clamped end of the wire. The following boundary conditions should be satisfied:

$$w(0) = 0, \, w'(0) = 0, \, w''(l) - 0,$$
$$EI w'''(l) + T w'(l) + P - 0. \tag{18.B2}$$

In order to satisfy the four conditions (18.B2), the Equation (18.B1) is differentiated twice, and the solution to the obtained differential equation of the fourth order is as follows:

$$w(x) = C_0 + C_1 kx + C_2 \cos kx + C_3 \sin kx, \tag{18.B3}$$

where

$$k = \sqrt{\frac{T}{EI}} \tag{18.B4}$$

is the parameter of the compressive force. Introducing the solution (18.B3) into the boundary conditions (18.B2), we find:

$$C_0 = -C_2 = \frac{P}{kT} \tan kl,$$
$$C_1 = -C_3 = -\frac{P}{kT}, \tag{18.B5}$$

and the solution (18.B3) results in the following expression for the deflection function:

$$w(x) = \frac{P}{kT} \left\{ \tan kl - kx - \frac{\sinh[k(l-x)]}{\cosh kl} \right\}. \tag{18.B6}$$

The maximum deflection at the wire end is

$$w(l) = \frac{P}{kT} (\tan kl - kl). \tag{18.B7}$$

The maximum deflection at the free end of a cantilever beam subjected to a lateral force P applied at this end is

$$\delta = \frac{Pl^3}{3EI}. \tag{18.B8}$$

Comparing the Equations (18.B5) and (18.B6), we conclude that the parameter

$$\varsigma = 3 \frac{\tan kl - kl}{(kl)^3} \tag{18.B9}$$

considers the effect of the axial compression on the lateral compliance of a cantilever wire ("beam"). Within the framework of the linear approximation, the parameter ς is infinitely

large, when the compressive force, T, reaches its critical (Euler) value. Indeed, this parameter is infinitely large, when $kl \to \pi/2 = 1.571$. In this case the Equation (18.B3) yields

$$T = \frac{\pi^2 \cdot EI}{4l^2},$$

which is a well known expression for a critical force for a cantilever beam. But even when the parameter kl is only $kl = 0.866$, the parameter ς is as high as about 6.4, and in such a case a 2.5 fold decrease in the interfacial shearing stress could be expected. Thus, there is a definite incentive, as far as the interfacial shearing stress is concerned, for using nanowire-based bonding structures subjected to compression.

APPENDIX 18.C. COMPRESSIVE FORCES IN THE NPM-BASED COMPOUND STRUCTURE

The desirable compression in the compound structure could be achieved by application of external forces, but it certainly can stem from the bonding compound features, as quantitatively shown below.

Let us define the system parameters as following:
S_S overall are of surfaces to be bonded,
S_B interfacial area of contact between the bonded surface and bonding compound,
S_C side area of the compound (in contact with air),
σ_{SA} interfacial tension coefficient between the bonded surface and air,
σ_{SC} interfacial tension coefficient between the bonded surface and the compound,
σ_{CA} interfacial tension coefficient between the compound and air,
d gap between the bonded surfaces,
R_C radius of the contact area,
and
V_C volume of the compound located between the bonded surfaces.

Constraint of the compound volume conservation during any spread/wetting process should be considered in the expression for the system surface tension energy:

$$E = 2 \cdot \sigma_{SA} \cdot (S_S - S_B) + \sigma_{CA} \cdot S_C + 2 \cdot \sigma_{SC} \cdot S_B$$

provided

$$S_B \cdot d = V_C. \tag{18.C1}$$

It is clear that

$$S_B = \pi \cdot R_C^2,$$

and

$$S_C = 2 \cdot \pi \cdot R_C \cdot d. \tag{18.C2}$$

Then, the system energy can be easily expressed vs. d or S_B. Let us bring the dependence of this energy on the contact area S_B:

$$E(S_B) = 2 \cdot \left[\sigma_{SA} \cdot S_S + \sigma_{CA} \cdot \frac{V_C \cdot \sqrt{\pi}}{\sqrt{S_B}} + (\sigma_{SC} - \sigma_{SA}) \cdot S_B \right]. \tag{18.C3}$$

In a case of $\sigma_{SC} < \sigma_{SA}$ there the energy function does not have any minimum, and the system tends to the complete bonded surface coverage with the compound, and the equilibrium is achieved only with the help of repulsive forces provided by the nanowires, microspheres and other embedded "elastic" elements. On the other hand, in an opposite case, when $\sigma_{SC} > \sigma_{SA}$, the energy has a minimum at

$$S_B = \sqrt[3]{\frac{\pi \cdot V_C^2}{4} \cdot \frac{\sigma_{SC}^2}{(\sigma_{SC} - \sigma_{SA})^2}},$$

or

$$d = \sqrt[3]{\frac{4 \cdot V_C}{\pi} \cdot \frac{(\sigma_{SC} - \sigma_{SA})^2}{\sigma_{SC}^2}}. \tag{18.C4}$$

As a quasi-elastic system (actually, visco-elastic system), this system tries to achieve a state of equilibrium that corresponds to the minimum of the elastic energy associated with surface tension and the nanowires buckling and microspheres compression. Then the system will operate in the condition of a dynamic steady-state (stable) equilibrium with the "distractive" reactive forces caused by the compressed nano-wires and the compression forces of the surfaces tension.